Nuclear Engineering and Technology 48 (2016) 1330–1337

Available online at ScienceDirect

Nuclear Engineering and Technology

journal homepage: www.elsevier.com/locate/net

Original Article

Fuel–Coolant Interaction Visualization Test for In-Vessel Corium Retention External Reactor Vessel Cooling (IVR-ERVC) Condition

Young Su Na[*], *Seong-Ho Hong*, *Jin Ho Song*, *and Seong-Wan Hong*

Severe Accident and PHWR Safety Research Division, Korea Atomic Energy Research Institute, 989-111 Daedeok-daero, Yuseong-gu, Daejeon 305-353, South Korea

ARTICLE INFO

Article history:
Received 5 October 2015
Received in revised form
17 March 2016
Accepted 8 June 2016
Available online 1 July 2016

Keywords:
Fuel–Coolant Interaction
Severe Accident
Steam Explosion
Test for Real cOrium Interaction with water (TROI)

ABSTRACT

A visualization test of the fuel–coolant interaction in the Test for Real cOrium Interaction with water (TROI) test facility was carried out. To experimentally simulate the In-Vessel corium Retention (IVR)- External Reactor Vessel Cooling (ERVC) conditions, prototypic corium was released directly into the coolant water without a free fall in a gas phase before making contact with the coolant. Corium (34.39 kg) consisting of uranium oxide and zirconium oxide with a weight ratio of 8:2 was superheated, and 22.54 kg of the 34.39 kg corium was passed through water contained in a transparent interaction vessel. An image of the corium jet behavior in the coolant was taken by a high-speed camera every millisecond. Thermocouple junctions installed in the vertical direction of the coolant were cut sequentially by the falling corium jet. It was clearly observed that the visualization image of the corium jet taken during the fuel–coolant interaction corresponded with the temperature variations in the direction of the falling melt. The corium penetrated through the coolant, and the jet leading edge velocity was 2.0 m/s. Debris smaller than 1 mm was 15% of the total weight of the debris collected after a fuel–coolant interaction test, and the mass median diameter was 2.9 mm.

1. Introduction

Fuel–Coolant Interaction (FCI) can threaten the reactor cavity integrity during a severe accident. Thermal energy transfer from a high-temperature molten core material to coolant water within a short time causes a mechanical energy output, i.e., dynamic pressure, which applies force to damage the surrounding structures. When the corium melt penetrates into the coolant, the film boiling induced by the high temperature difference between the water and the melt jet generates steam. The hydrodynamic instabilities created by the differences of velocity and density as well as the vapor production break up the melt into fragments of the size of a few millimeters. The melt jet, particles, water, and steam exist together. The corium jet penetrating into water remains in a liquid phase because the vapor acts as a thermal resistance layer that reduces the heat transfer between the corium and the coolant. Solidification of corium in the liquid state can be delayed by a thermal

* *Corresponding author.*
E-mail address: ysna@kaeri.re.kr (Y.S. Na).
http://dx.doi.org/10.1016/j.net.2016.06.010

resistance layer. A local explosion of a single fragment or a small group of fragments can go through the entire melt. This weak explosion can trigger a steam explosion in the total mixing zone. A local explosion can also occur when the front of the melt comes in contact with the bottom surface of the cavity [1]. The pressure wave from the trigger penetrates into and expands through the falling melt, and locally removes the vapor film around the fragments that break up into a micro size. A rapid heat transfer between the corium and the coolant makes explosive vaporization. In summary, steam explosions can occur sequentially during premixing, triggering, propagation, and expansion. Previous experimental studies regarding FCI have been conducted under a free fall of the corium melt in a gas phase before making contact with the coolant water [2–4]. They simulated the molten corium injecting from the reactor vessel failure to a cavity partially filled with water. There are free fall distances, as one of the experimental conditions shown in Table 1, in the test facilities such as Furnace And Release Oven (FARO), KROTOS, and Test for Real cOrium Interaction with water (TROI). All tests used a prototypic corium including uranium oxide (UO_2) and zirconium oxide (ZrO_2) with a weight ratio of 8:2. While there were no spontaneous steam explosions in the test cases L-29, L-31, and K-56, a steam explosion occurred in K-58 and TROI-37, which had an artificial external trigger. In the results of TROI-37, the average melt speed in the coolant was 2.0 m/s and the cumulative mass fraction of particles smaller than 1 mm was 64%.

The previous FCI test conditions including free fall distances are different from an In-Vessel corium Retention External Reactor Vessel Cooling (IVR-ERVC) case, which makes the cavity flood, i.e., there is no free fall distance between the reactor vessel and the coolant. In a new-generation reactor such as the Advanced Power Reactor 1400, IVR-ERVC has been adopted as a mitigation strategy for a severe accident [5]. The corium melts release directly into the coolant water without a free fall distance in a gas phase when vessel failure occurs under the IVR-ERVC conditions. It is expected that the free fall conditions can accelerate a corium jet falling in a gas, and then the fast inlet velocity of a jet entering into a water pool can reduce the diameter of the melt drops. This relationship between a jet velocity and a drop size was confirmed by a numerical analysis using the TRansient Analysis Code for Explosive Reactions (TRACER-II) [6]. In addition, the jet leading edge velocity in water for a condition excluding a free fall distance was calculated to be about 3.0 m/s, which was close to that including a free fall distance of 3 m. To the best of our knowledge, there have been no experimental studies on the FCI under IVR-ERVC conditions to date. In order to overcome the lack of experimental data, we carried out a visualization test on the interaction of corium and coolant water in a condition excluding a free fall distance of a melt jet in a gas phase before making contact with water. The jet leading edge velocity and the size distribution of debris were evaluated in this study. A previous version of this article was presented at the 9th Korea–Japan Symposium on Nuclear Thermal Hydraulics and Safety, November 18, 2014 [7].

Table 1 – Experimental conditions of some previous FCI tests.

Experimental conditions	FARO[a]	KROTOS[b]	TROI[c]
Melt mass (kg)	39 and 92	4 and 3.6	20
Melt jet diameter (mm)	50	30	80
Free fall distance in a gas (m)	0.74 and 0.77	0.32 and 0.42	3.55
Pool depth (m)	1.48 and 1.45	0.975 and 0.917	0.95
Water subcooling (K)	97 and 104	123 and 125	60

[a] Test cases: L-29 and L-31 [2].
[b] Test cases: K-56 and K-58 [3].
[c] Test cases: TROI-37 [4].
FARO, Furnace And Release Oven; FCI, Fuel–Coolant Interaction; TROI, Test for Real cOrium Interaction with water.

2. Materials and methods

2.1. TROI test facility

The TROI test facility [4, 8] was modified to simulate the IVR-ERVC conditions, as shown in Fig. 1. To remove the free fall distance in a gas phase, the corium melt is kept briefly in the intermediate catcher located just above the water level in the interaction vessel. The TROI test facility consists of the following two vessels:

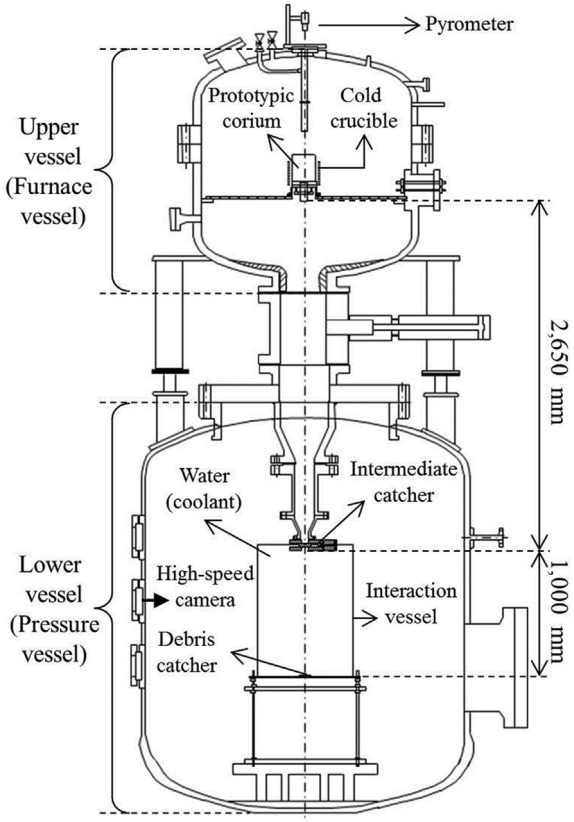

Fig. 1 – TROI test facility to observe the FCI in the IVR-ERVC condition. FCI, Fuel–Coolant Interaction; IVR-ERVC, In-Vessel corium Retention External Reactor Vessel Cooling; TROI, Test for Real cOrium Interaction with water.

(1) The upper vessel, called the furnace vessel, contains a cold crucible to make the superheated corium melt.
(2) The lower vessel, called the pressure vessel, includes an interaction vessel filled with subcooled water to observe the FCI.

The furnace vessel is connected with the pressure vessel in a normal direction with the same center. Fig. 2 shows that a square interaction vessel, 600 mm in length and 1,200 mm in height, has three transparent side surfaces for the visualization test. The temperature variations in time and direction of a falling melt jet were measured using 25 thermocouples. The K-type thermocouple junctions within the water were fixed on a cylindrical steel support (400 mm in diameter and 800 mm in height). Junctions were positioned in a 100-mm-diameter in the center of an interaction vessel, indicated as A, B, C, D, and E, as shown in Fig. 2, where the C position is the center of the interaction vessel. We located the five thermocouple junctions (A–E) at each of the five elevations of 0 mm, 200 mm, 400 mm, 600 mm, and 800 mm from the bottom of the interaction vessel. The maximum measurable temperature of the K-type thermocouple is 1,250°C. The response time of the probe thermocouple with a diameter of 0.5 mm was about 0.25 seconds in water. It is expected that 25 sacrificial thermocouples installed in the vertical direction of the coolant can be cut by the corium that has a high temperature of more than 2,000°C. The temperature increment in time measured by the sacrificial thermocouples can show that the corium melt front goes through the coolant. We also observed the jet penetration during the FCI using a high-speed camera, and this visualization image was compared with the temperature variation in time. A high-speed camera (Phantom Miro3; Vision Research, Wayne, NJ, USA) focusing on sides A and B in Fig. 2 recorded the behavior of the corium melt penetrating through water. In addition, we measured static pressure over time in the TROI test facility using pressure transducers (PA23S; Keller, Winterthur, Switzerland).

2.2. *Experimental procedure*

This visualization test proceeded sequentially as follows:

(1) Making the corium melt: the mixture of the UO_2 pellets and ZrO_2 powder with a weight ratio of 80:20 (UO_2:ZrO_2) was charged in a cold crucible to make 34.39 kg of the prototypic corium. The corium melt was generated using the induction heating (150 kW in power and 50 kHz in frequency) method [9]. In the melting process, a two-color optical pyrometer (3R-35C15-0-0-0-1; IRCON, Santacruz, CA, USA) measured the temperature of the top surface of the corium melt to confirm the superheated quality. Dangerous factors such as aerosol generated in the melting process and the high-temperature corium were blocked by the furnace vessel of the TROI test facility.
(2) Delivering the corium melt: a releasing hole, 100 mm in diameter, at the bottom of the cold crucible was blocked by a cylindrical plug with a cooling system. A thin crust layer at the bottom of a crucible was created in the melting process. The plug blocking the releasing hole was removed, and a puncher broke the thin crust layer at the bottom of the crucible when the melt temperature, measured by an optical pyrometer, approached the desired value. Finally, the corium melt dropped on the intermediate catcher located just above the water level, and the melt was kept briefly in the catcher to remove the free fall distance in a gas phase before making contact with the coolant.
(3) Interaction of the corium melt with the coolant: the corium melt penetrated through water in the interaction vessel when the intermediate catcher had opened 50 mm in diameter. The pressure vessel in the TROI test facility was designed for experimental safety in case of a possible steam explosion. The sacrificial thermocouples measured the temperature increment in time and in the vertical direction of the water owing to the melt jet penetration through the coolant. We observed the FCI by both images taken using the high-speed camera and the temperature variations measured by the sacrificial thermocouples. The recording time of the high-speed camera was synchronized with that of the sacrificial thermocouples when the intermediate catcher opened.
(4) Debris analysis: the debris collected in the debris catcher in the TROI test facility was dried in an oven after the FCI test. We estimated the size distribution of sieved debris as the evidence of a steam explosion. The

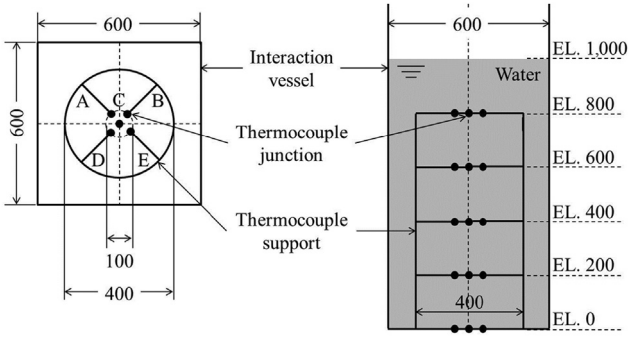

Fig. 2 – Twenty-five thermocouple junctions in the interaction vessel. EL, elevation.

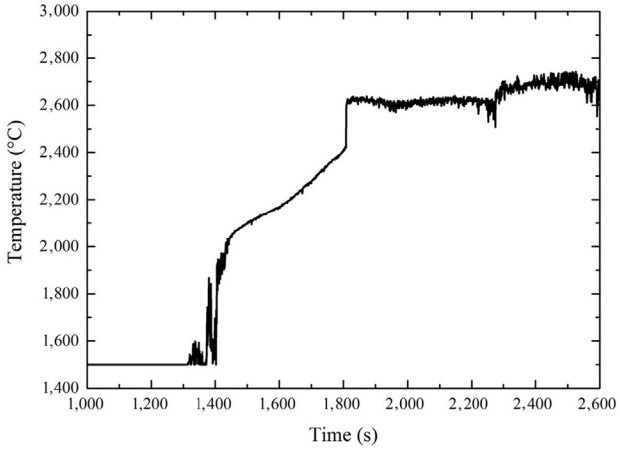

Fig. 3 – Temperature of the top surface of a corium melt in a cold crucible.

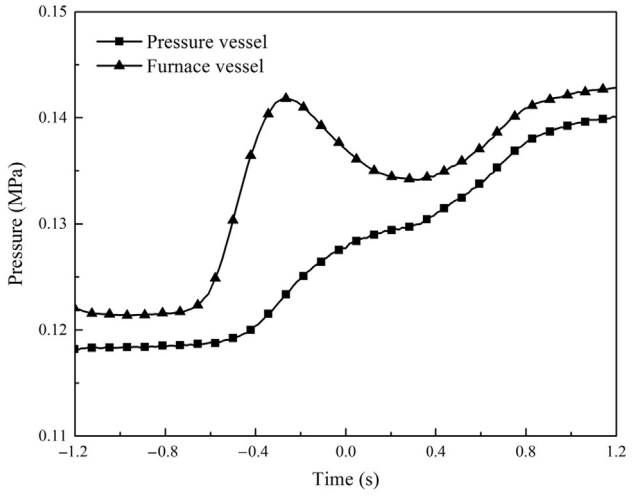

Fig. 4 – Static pressure in the pressure (lower) and furnace (upper) vessels.

inductively coupled plasma atomic emission spectrometry measured the debris composition, which was compared with the weight ratio of UO_2 and ZrO_2 of the initial charging mass.

3. Results and discussion

3.1. *Corium melt*

In the melting process, the temperature of the top surface of the corium melt in the cold crucible was measured by an optical pyrometer, as shown in Fig. 3. The temperature started to increase at about 1,400 seconds after the operation of the induction heating, and increased rapidly from about 2,430°C to 2,630°C at 1,800 seconds. This temperature jump could be explained by the phase change from the solid to the liquid phase on the top surface of the charged mixture of UO_2 and ZrO_2. The melting temperature of the prototypic corium with a weight ratio of UO_2 to ZrO_2 of 80:20 is expected to be about 2,577°C from the phase diagram [10]. The temperature of 2,630°C measured at 1,800 seconds is higher than the melting temperature of 2,577°C. The fluctuation of the measured temperature became stronger after 2,500 seconds because the aerosol generated by the corium melt interrupted the temperature measurement of the optical pyrometer [9]. Argon gas was injected into the focus area of the optical pyrometer to remove the aerosol. The top surface temperature of the corium melt was maintained at 2,630°C from about 1,800 seconds to 2,275 seconds, and the temperature then increased up to about 2,730°C. The prototypic corium superheated in a cold crucible fell on the intermediate catcher located just above the water level. The melt was kept briefly in the catcher before making contact with the coolant. We measured the static pressure over time in the TROI test facility consisting of the upper vessel and the lower vessel, called the furnace vessel and the pressure vessel, respectively, as shown in Fig. 4. The recording time of the pressure was zero when the intermediate catcher had opened. The pressure in the furnace vessel increased at about −0.6 seconds in Fig. 4, because the high-temperature corium melt had expanded the atmosphere in the furnace vessel during the corium transfer. The pressure in the lower vessel of the TROI test facility started to increase at about −0.4 seconds when the corium was close to the intermediate catcher. The corium transfer nozzle inside the lower vessel has holes to prevent an overpressure in the vicinity of the intermediate catcher. The corium melt penetrated into the coolant when the intermediate catcher opened at about 0.0 seconds. In Fig. 4, the pressure in the upper and lower vessels increased simultaneously because of the steam generation during the FCI.

3.2. *Fuel–coolant interaction*

Figs. 5–9 show the temperature variations measured by the sacrificial thermocouples installed in the vertical direction of the coolant and a visualization image taken by a high-speed camera during the FCI. The recording time of the thermocouples was synchronized with that of the visualization test as soon as the intermediate catcher opened. A, B, C, D, and E indicate the positions of thermocouple junctions at each elevation; there are five elevations starting from the bottom of the interaction vessel, as shown in Fig. 2. As seen in Fig. 5, the

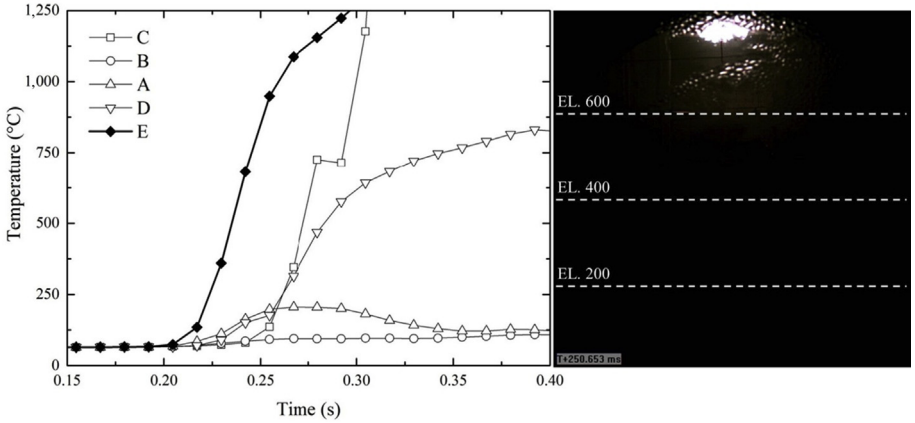

Fig. 5 – Temperature measured at EL. 800 mm and high-speed camera image at 0.25 seconds. EL, elevation.

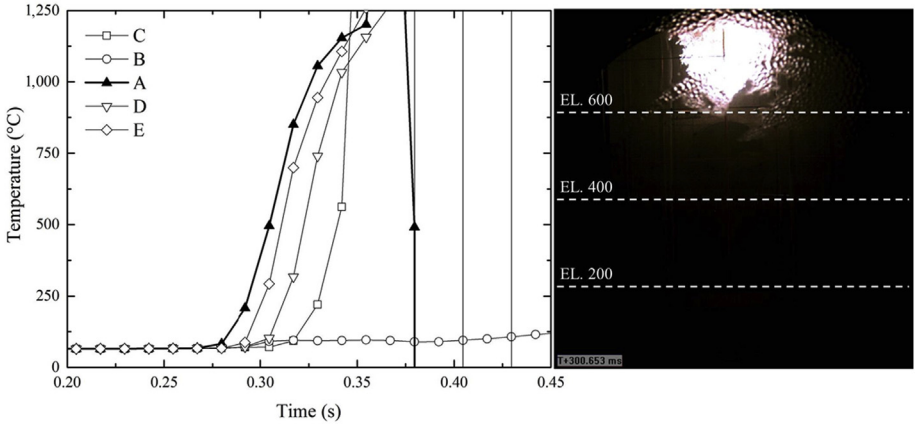

Fig. 6 – Temperature measured at EL. 600 mm and high-speed camera image at 0.30 seconds. EL, elevation.

melt jet passed an elevation of 800 mm at about 0.25 seconds after the opening of the intermediate catcher. Although the five thermocouple junctions from A to E were positioned at the same elevation of 800 mm, the junction at the E position, indicated as a solid symbol in Fig. 5, was cut first due to the high-temperature melt jet. It seems that the corium leading edge passed the elevation of 800 mm in the E–C direction because the thermocouple junctions installed at the A and B positions were not disconnected. The temperature variation in Fig. 5 shows the unexpected decrement at the C position. It is expected that the direction of a falling melt jet can suddenly change due to hydrodynamic instabilities. Fig. 6 shows the temperature variation measured at an elevation of 600 mm and the visualization image taken at 0.30 seconds. The thermocouple junction at the A position was disconnected first. It seems that the melt front was not going through the B direction at the elevation of 600 mm. The fluctuated temperature signal after initially approaching the maximum temperature of 1,250°C can be generated from the rewetted thermocouple junction owing to high-temperature corium. The melt jet penetrated at an elevation of 400 mm at about 0.40 seconds, as shown in Fig. 7. The thermocouple junction at the D position, indicated as a solid symbol, was cut first, even though the five junctions from A to E were located at the same elevation of 400 mm. The melt jet front approached the elevation of 400 mm in the D–C direction. Fig. 8 indicates that the corium went through an elevation of 200 mm at about 0.55 seconds. The thermocouple junction at the E position was disconnected first. It seems that the melt front was not passing in the B direction at an elevation of 200 mm. Finally, the corium melt injected from the intermediate catcher right above the water level approached the bottom of the interaction vessel at about 0.60 seconds, as shown in Fig. 9. The corium melt penetrated a 1,000-mm-high water pool in about 0.60 seconds after the opening of the intermediate catcher. Fig. 10 shows the temperature variations measured at each elevation from 800 mm to the bottom of the interaction vessel, where the junction positions indicated in parentheses imply the first to reach the elevation, as indicated by the solid symbols in Figs. 5–9. We can observe that the sacrificial thermocouples installed from 800 mm to the bottom of the interaction vessel were cut sequentially by the falling corium. The melt jet did not uniformly penetrate through water due to hydrodynamic instabilities. We can estimate the jet leading edge penetrating into water in the vertical direction over time, as shown in Fig. 11. The leading edge velocity was about 2.0 m/s, where the horizontal bars indicate the time taken from the initial temperature to the maximum temperature of 1,250°C. The leading edge velocity was calculated from 800 mm to the bottom of the test vessel, as shown in Fig. 11. In this study, a corium jet was observed to fall in water at a constant rate of 2.0 m/s. A test case [11] in a condition including a free fall distance also shows a

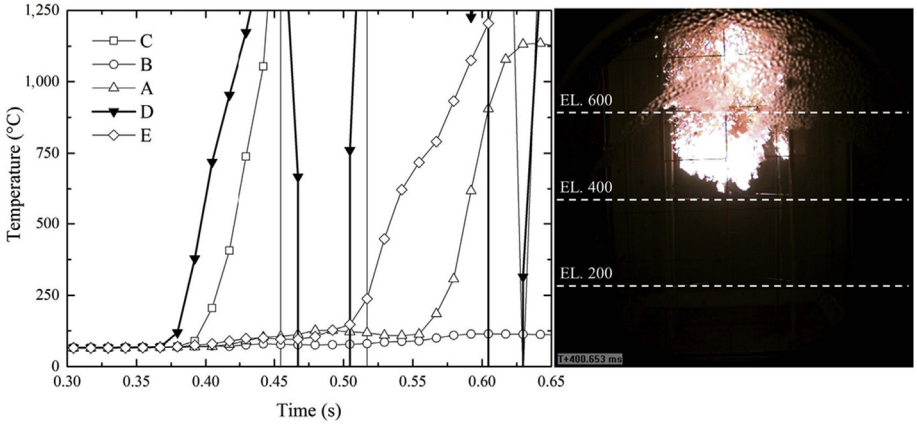

Fig. 7 – Temperature measured at EL. 400 mm and high-speed camera image at 0.40 seconds. EL, elevation.

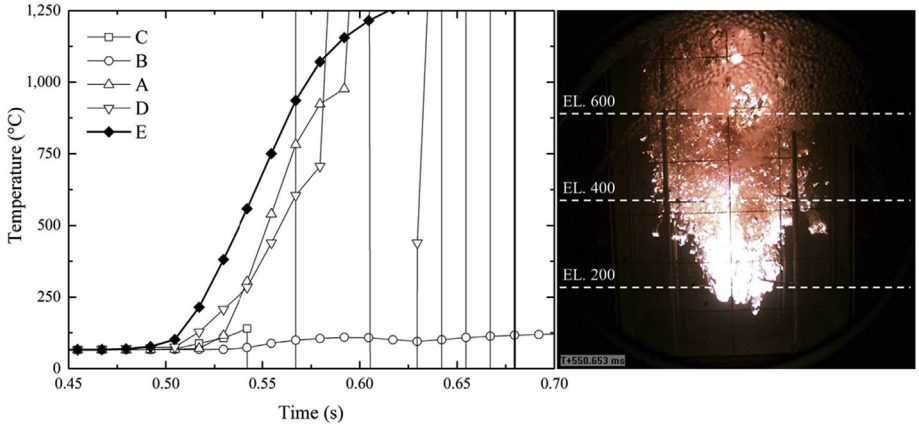

Fig. 8 – Temperature measured at EL. 200 mm and high-speed camera image at 0.55 seconds. EL, elevation.

constant jet velocity in a coolant when the jet breakup length is longer than the water depth. In the previous numerical analysis [6] using the TRACER-II code, the melt front velocity for a case excluding a free fall distance in a gas phase was calculated similarly to that including a free fall distance of 3 m. In addition, the leading edge velocity of 2.0 m/s in this study was found to be close to that found in the previous TROI test conditions including free fall distances of 2.75 m and 3.55 m [4]. It seems that the effect of a free fall distance on the leading edge velocity is minor, even though the initial velocity of a corium jet entering the water surface is accelerated by a free fall. However, from one test case excluding a free fall distance, it is difficult to conclude the relation between a free fall distance and the jet leading edge velocity in water. The leading edge velocity can be affected by various experimental conditions. Further studies excluding a free fall distance are necessary.

3.3. *Debris analysis*

The occurrence of the steam explosion can be assured by the size distribution of debris, which presents the degree of breakup during the FCI. The 22.54 kg of debris collected from the debris catcher at the bottom of the interaction vessel was dried in an oven. The initial charging weight of 34.39 kg decreased by about 34% in the collected debris because some corium remained in the cold crucible and it had deposited on the nozzle inner wall during melt delivery. Fig. 12 shows the size distribution of the sieved debris. The cumulative mass fraction of particles smaller than 1 mm was 15%, and the mass median diameter was 2.9 mm. In this study, no steam explosion was observed in the high-speed camera images, as shown in Figs. 5–9, and this nonexplosion was also confirmed by the dynamic pressure of zero measured on the interaction vessel wall during the FCI. Previous studies in a condition including free fall distances in a gas phase concluded that the debris size for the case of a steam explosion is smaller than that for a nonexplosion [8, 11]. In the steam explosion of the TROI test [8], the cumulative mass fraction of particles smaller than 1 mm is more than 60%, which is much higher than the value of 15% found in this study. At the same depth from the water surface, the average melt drop diameter for a condition excluding a free fall was calculated to be more than twice that for a case including a free fall distance of 3 m [6]. Unlike the numerical result mentioned above, it was experimentally observed that the mass median diameter of the sieved debris in this study was similar to that in the quenching result of the previous TROI

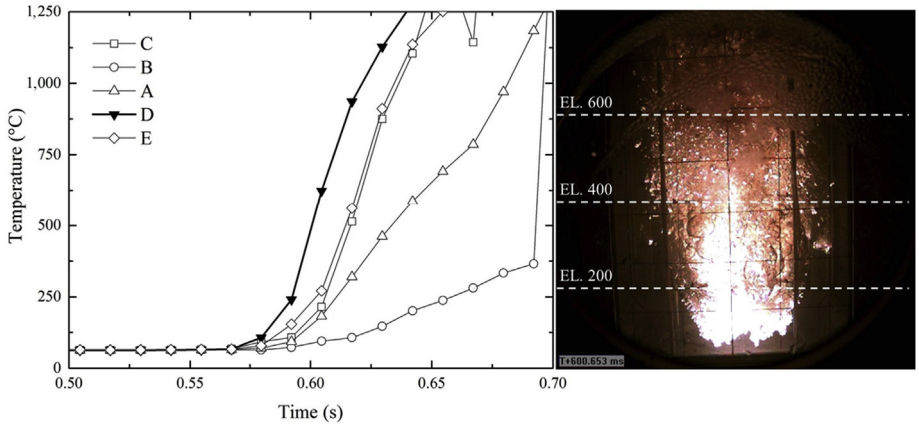

Fig. 9 – Temperature measured at the bottom of the interaction vessel and high-speed camera image at 0.60 seconds. EL, elevation.

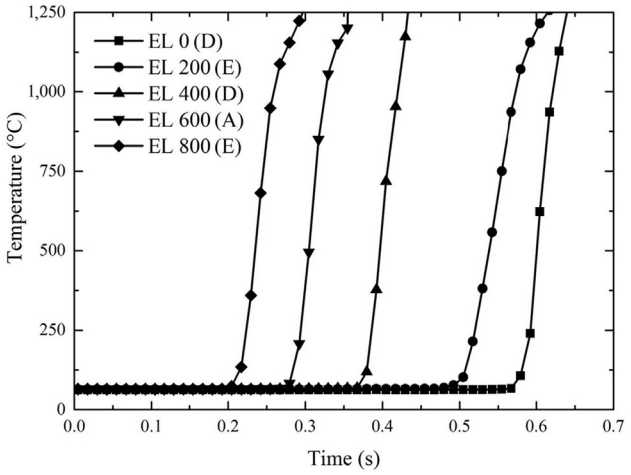

Fig. 10 – Temperature variations measured in the water depth. EL, elevation.

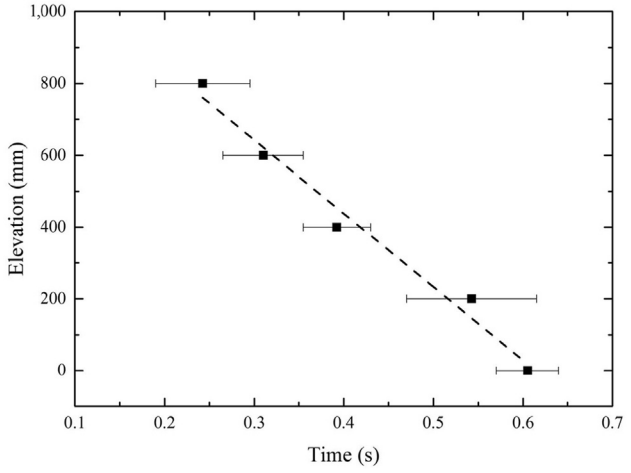

Fig. 11 – Jet leading edge penetrating through a coolant.

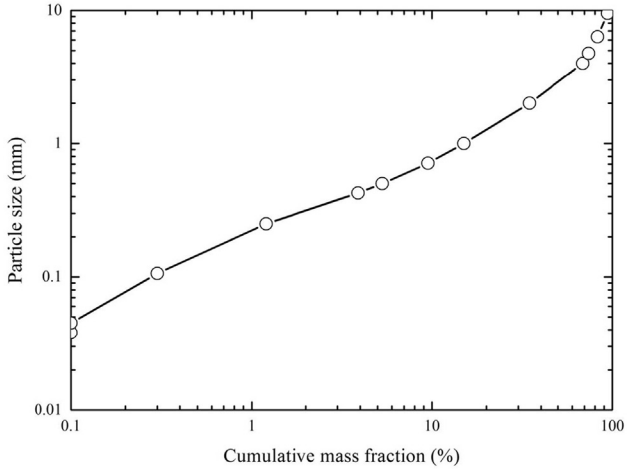

Fig. 12 – Size distribution of the debris.

test in a case including a free fall distance of 3.8 m [8]. It seems that there is little difference in the debris size according to whether or not there was a free fall. In a large-sized test simulating a complex physical phenomenon such as the FCI, it is difficult to explain the overall phenomenon from a few test cases because there are various impact factors in test conditions. A stochastic analysis of the sieved debris obtained in the various tests excluding a free fall distance is necessary.

The porosity measured by water filled into the debris pores was 46.01%. From the inductively coupled plasma atomic emission spectrometry analysis, the weight ratio of UO_2 and ZrO_2 in the debris was measured to be 79.43:20.57, which nearly matched the initial composition of the charging mass.

4. Conclusion

A visualization test of the FCI under the IVR-ERVC condition was carefully conducted in the TROI test facility. We removed the free fall distance of corium in the gas phase before making contact with cooling water to simulate the submerged reactor vessel in a cavity filled with water. Corium penetrating into water was measured by 25 sacrificial thermocouples installed in the direction of a falling melt jet within a coolant. The temperature variation during the FCI owing to jet penetration was compared with visualization images taken by a high-speed camera. Prototypic corium consisting of UO_2 and ZrO_2 at a weight ratio of UO_2 to ZrO_2 of 80:20 was heated up to 2,730°C using the induction heating method. The corium melt was delivered to the intermediate catcher located just above the water level, and it then remained for a short time before making contact with the coolant. It was observed that the corium melt penetrated into water to a depth of 1,000 mm, and it took about 0.6 seconds from the opening of the intermediate catcher. The jet penetration was also confirmed by the sequential temperature variation measured by the sacrificial thermocouples installed in the direction of a falling melt. The corium released into the center of the interaction vessel did not uniformly penetrate through water owing to hydrodynamic instability, and the jet leading edge velocity was calculated to be about 2.0 m/s, which is similar to the velocities shown in the previous TROI test including free fall distances of 2.75 m and 3.55 m. An amount of 22.54 kg of debris was collected after the FCI test, which was then dried in an oven. The cumulative mass fraction with a particle size of < 1 mm was 15%, and the mass median diameter was 2.9 mm, which indicated relatively large-sized debris compared with the case of a steam explosion. The mass median diameter of the sieved debris in this study was similar to that in the quenching result of the previous TROI test including a free fall distance of 3.8 m. It seems that the free fall distance has a very small effect on the debris size as well as the jet leading edge velocity. However, it is difficult to draw conclusions about the FCI under IVR-ERVC conditions from this one test case. An additional stochastic analysis of the sieved debris obtained in several conditions excluding a free fall distance is necessary because there are various factors, such as melting temperature and compositions of prototypic corium, in the large-sized FCI test. A TROI visualization test can generate valuable information on the behavior of a corium melt jet and the

premixing phase, as an initial condition of steam explosion, to validate the computer code, even though there are differences between test conditions and real IVR cases, especially the effects of scale, water level, and break position. We should consider a real situation when we discuss the test results conducted under a limited condition. In this study, no spontaneous steam explosion was observed in the high-speed camera images, and this nonexplosion was also confirmed by the dynamic pressure of zero measured on the interaction vessel wall. Further studies on a steam explosion under IVR-ERVC conditions are necessary to compare with the dynamic load of a case including a free fall distance. It would be helpful to optimize a strategy for managing a severe accident.

Conflicts of interest

No conflicts of interest.

Acknowledgments

This work was supported by the National Research Foundation of Korea (NRF) grant funded by the Korean Government (Ministry of Science, ICT, and Future Planning; No. 2012M2A8A4025889).

REFERENCES

[1] B.R. Sehgal, Nuclear Safety in Light Water Reactors, Elsevier, Inc., Waltham, MA, USA, 2012, pp. 255–271.

[2] D. Magallon, I. Huhtiniemi, Corium melt quenching test at low pressure and subcooled water in FARO, Nucl. Eng. Des. 204 (2001) 369–376.

[3] I. Huhtiniemi, D. Magallon, Insight into steam explosions with corium melts in KROTOS, Nucl. Eng. Des. 204 (2001) 391–400.

[4] J.H. Kim, I.K. Park, B.T. Min, S.W. Hong, S.H. Hong, J.H. Song, H.D. Kim, Results of the triggered steam explosions from the TROI experiment, Nucl. Technol. 158 (2007) 378–395.

[5] R. Park, K.H. Kang, S.W. Hong, S.B. Kim, J.H. Song, Corium behavior in the lower plenum of the reactor vessel under IVR-ERVC condition: technical issues, Nucl. Eng. Technol. 44 (2012) 237–248.

[6] K.H. Bang, R. Kumar, H.T. Kim, Modeling corium jet breakup in water pool and application to ex-vessel fuel–coolant interaction analyses, Nucl. Eng. Des. 276 (2014) 153–161.

[7] Y.S. Na, S.W. Hong, J.H. Song, S.H. Hong, Pre-mixing visualization in fuel–coolant interaction without a free fall of the corium melt, 9th Korea–Japan Symposium on Nuclear Thermal Hydraulics and Safety, Buyeo, Korea, November 16–19, 2014.

[8] I.K. Park, J.H. Kim, B.T. Min, S.W. Hong, Thermal–hydraulic aspects of FCIs in TROI corium/water interaction, Nucl. Eng. Des. 263 (2013) 419–430.

[9] S.W. Hong, B.T. Min, J.H. Song, H.D. Kim, Application of cold crucible for melting of UO_2/ZrO_2 mixture, Mater. Sci. Eng. A357 (2003) 297–303.

[10] B.T. Min, S.W. Hong, J.H. Song, H.D. Kim, Thermophysical Properties of the Corium, KAERI/TR-2013/2002, Ch. 3, Korea Atomic Energy Research Institute, Daejeon, Korea, 2002.

[11] D. Magallon, Characteristics of corium debris bed generated in large-scale fuel–coolant interaction experiments, Nucl. Eng. Des. 236 (2006) 1998–2009.